ACS APPLIED MATERIALS & INTERFACES

Research Article

Cite This: ACS Appl. Mater. Interfaces 2018, 10, 28672−28678

www.acsami.org

Efficient Light Absorption by GaN Truncated Nanocones for High Performance Water Splitting Applications

Yeong Jae Kim,[†] Gil Ju Lee,[†] Seungkyu Kim,[‡] Jung-Wook Min,[§] Sang Yun Jeong,[‡] Young Jin Yoo,[†] Sanghan Lee,[‡] and Young Min Song*[,†]

[†]School of Electrical Engineering and Computer Science, Gwangju Institute of Science and Technology, 123 Cheomdangwagi-ro, Buk-gu, Gwangju 61005, Republic of Korea

[‡]School of Materials Science and Engineering, Gwangju Institute of Science and Technology, 123 Cheomdangwagi-ro, Buk-gu, Gwangju 61005, Republic of Korea

[§]Photonics Laboratory, King Abdullah University of Science and Technology (KAUST), Thuwal 23955-6900, Saudi Arabia

Supporting Information

ABSTRACT: Despite the importance of gallium nitride (GaN) nanostructures for photocatalytic activity, relatively little attention has been paid to their geometrical optimization on the basis of wave optics. In this study, we present GaN truncated nanocones to provide a strategy for improving solar water splitting efficiencies, compared to the efficiency provided by the conventional geometries (i.e., flat surface, cylindrical, and cone shapes). Computational results with a finite difference time domain (FDTD) method and a rigorous coupled-wave analysis (RCWA) reveal important aspects of truncated nanocones, which effectively concentrate light in the center of the nanostructures. The introduction of nanostructures is highly recommended to address the strong light reflection of photocatalytic materials and carrier lifetime issues. To fabricate the truncated nanocones at low cost and with large-area, a dry etching method was employed with thermally dewetted metal nanoparticles, which enables controllability of desired features on a wafer scale. Experimental results exhibit that the photocurrent density of truncated nanocones is improved about three times higher compared to that of planar GaN.

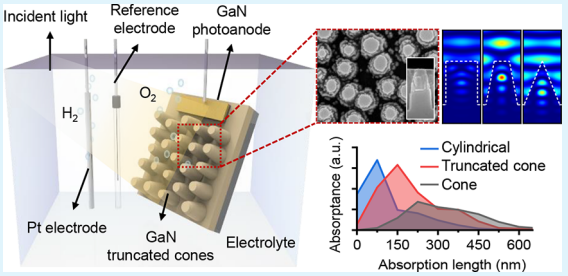

KEYWORDS: *gallium nitride, photoanode, light trapping, photon management, solar water splitting*

INTRODUCTION

As environmental problems such as global warming and air pollution arise due to fossil fuel-based energy production, the need for renewable and alternative energy development has been emphasized. Recently, solar water splitting, which exploits the reaction phenomenon between a photoelectrode material and water under solar irradiance, is one of the promising candidates for generating hydrogen in an ecofriendly manner.[1−3] In particular, hydrogen energy has garnered a great deal of attention as the next ideal generation alternative energy for zero emission. Various photoanode materials such as titanium oxide (TiO_2),[4,5] zinc oxide (ZnO),[6,7] tungsten oxide (WO_3),[8,9] α-iron oxide (Fe_2O_3),[10] and so forth have been used. These conventional materials exhibit weak points, however, such as difficulty to tune the band gap energy, low charge carrier mobility, and chemical corrosion in acid and alkali conditions. On the other hand, III-nitride materials can overcome these limitations due to their tunable band gap, a proper band edge position, outstanding electrical features, and good chemical stability.[11−13] So far, gallium-nitride (GaN) based studies have been performed on various powder, rod, and porous structures to increase active surface area and improve charge carrier separation efficiency.[14−17] However, there remains a major problem regarding optical aspects. Especially, a large amount of light reflection at high refractive index leads to optical losses in solar devices and an uncontrolled optical path for light absorption gives rise to charge carrier recombination by a limited diffusion length.[15,16] To overcome these optical drawbacks on GaN-based systems, several nanostructures have been suggested with enhancement of photon energy utilization above band gap energy.[18−21] Nevertheless, further research using wave optical simulation is emphasized to optically optimize nanostructures for reducing surface reflections with shortened optical absorption paths for photocatalytic water splitting applications.

Here, we present truncated nanocone structures on GaN as an optimal design to improve photocatalytic efficiency. In the process, we performed a parametric study to spectrally analyze the absorption of three representative nanostructures (i.e., cylindrical, truncated cone, and cone) for core structural parameters (i.e., period, height, and filling fraction) based on a rigorous coupled wave analysis (RCWA). In addition, we also

Received: June 1, 2018
Accepted: August 7, 2018
Published: August 7, 2018

DOI: 10.1021/acsami.8b09084
ACS Appl. Mater. Interfaces 2018, 10, 28672−28678

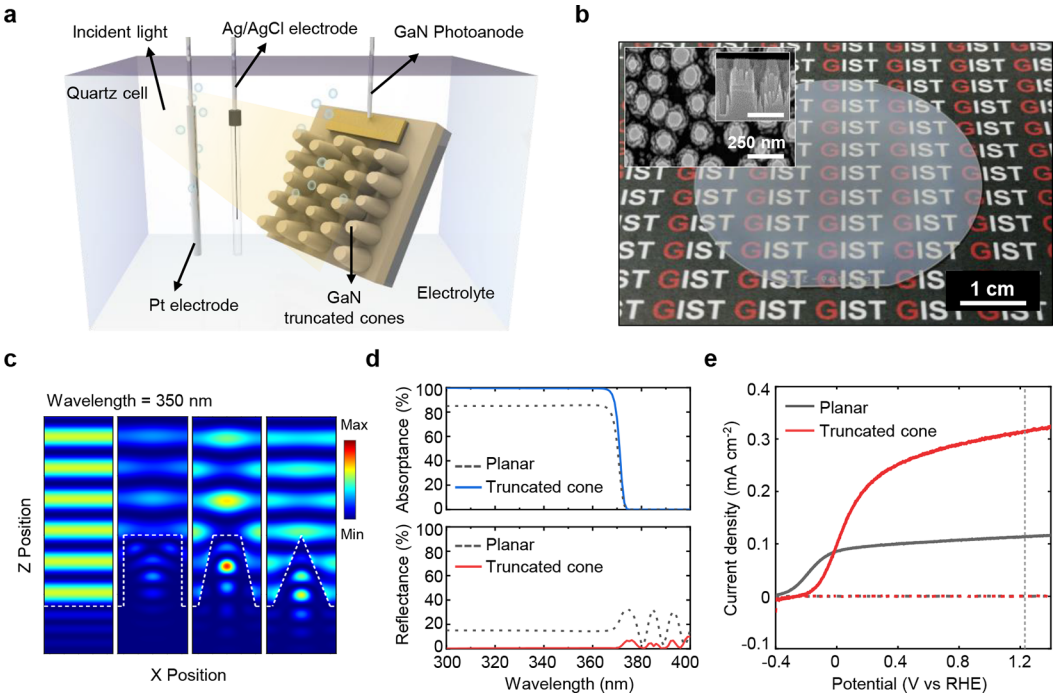

Figure 1. (a) A schematic diagram of photoelectrochemical cell. (b) A Photograph and SEM image (inset) of GaN truncated nanocones on a 2 in. sapphire substrate fabricated by 15 min etched SiO_2 mask. (c) Three dimensional finite-difference time-domain simulations for electric field distribution of planar, cylindrical, truncated cone, and cone. (d) Simulation results of absorptance/reflectance spectra of planar and truncated cone. (e) Photoelectrochemical measurements of planar and truncated nanocones.

evaluated the absorption depth for varying the cone ratio through a finite difference time domain (FDTD) method to determine the optimal nanostructure for water splitting applications. These theoretical analyses reveal that the truncated nanocone is appropriate for light trapping on the nanostructure near the electrolyte for reducing the moving path of generated carriers. This shortened path addresses carrier lifetime issues, ultimately increasing the overall photocatalytic reaction.[17,22] Based on these quantitative theoretical analyses, we exploited a mask-free surface texturing method through metal thermal dewetting and top-down etching process for fabrication of the truncated nanocones.[23,24] Via repetition of this consecutive fabrication step, the optimum GaN structure was found by optical, electrical, and photocatalytic characterizations such as reflectance, current density, incident photon-to-current conversion efficiency (IPCE), and electrical impedance spectroscopy (EIS) measurements.

EXPERIMENTAL SECTION

Optical Simulation. Numerical simulations for a rigorous coupled-wave analysis (RCWA) and finite-difference time-domain (FDTD) method were performed to calculate the electric field distribution and absorption spectra/profiles for the GaN materials respectively using commercial software (Diffract MOD, FullWAVE, RSoft Design Group). In the RCWA calculation, a fifth diffraction order and a grid size of 3 nm and periodic boundary conditions were used to calculate the diffraction efficiency. The unpolarized light absorption was calculated by averaging the TM and TE polarization. In the FDTD simulations, the simulation domain sizes in the *x*, *y*, and *z* directions were 3 nm and periodic boundary conditions were used for the large area of the computational regions. The GaN nanostructures were illuminated by a normal incident plane wave with 350 nm wavelength. Material dispersions and extinction coefficients were considered in the numerical simulations to observe exact optical properties. The optical constants of GaN and sapphire were taken from the UV−visible spectrometer and the electrolyte is considered as water.

Optical Characterization. To confirm the GaN truncated nanocones, field emission scanning electron microscopy (FE-SEM, Hitachi S-4700) was employed. A UV−visible spectrometer (Varian Cary 500 scan spectrophotometer) was used to measure the reflectance of the GaN samples.

Gallium Nitride Epitaxial Growth. GaN epilayers were grown on a c-plane sapphire substrate by metal organic chemical vapor deposition (MOCVD). The structure consists of a 30 nm GaN nucleation layer, a 500 nm undoped GaN (u-GaN) buffer layer, and a 1.5 μm top Si-doped GaN (n-GaN) layer. Typical electron concentration of the n-GaN layer is 5×10^{18} cm^{-3} with a mobility of ~200 cm^2 V^{-1} s^{-1} measured by using Hall effect measurements.

Photoelectrochemical cell (PEC) Measurements. PEC measurements were performed under an illuminated condition of 1 sun (100 mW cm^{-2}) using a 300 W Xe lamp (Newport) with an AM 1.5G filter (Newport). To measure the PEC properties of the GaN photoanodes, Ti/Au (10/150 nm) metal contacts were deposited onto the edge of GaN samples, and then the photoanode substrates were sealed with epoxy for insulation from the electrolyte, the area of exposed GaN samples was measured (ImageJ software). The light was illuminated on the front side GaN of the sample in a quartz cell with a three-electrode configuration. In our configuration, the GaN sample was used as a working electrode, whereas Pt and Ag/AgCl (saturated KCl) were employed as a counter electrode and a reference electrode, respectively. The potential applied on the GaN electrode was measured by Ag/AgCl (saturated KCl) and calculated from the potential versus the reversible hydrogen electrode (V vs RHE) through the following equation:

$$V_{RHE} = V^0{}_{Ag/AgCl} + V_{Ag/AgCl} + 0.059pH \quad (1)$$

where $V^0{}_{Ag/AgCl}$ is 0.197 V at 25 °C.

Aqueous solutions of 0.1 M potassium phosphate monobasic (KH_2PO_4, ≥ 99%, Aldrich) with 0.1 M potassium phosphate dibasic (K_2HPO_4, ≥99%, Aldrich) were introduced as the electrolyte (pH 7.0). Linear sweep voltammetry measurements and EIS were

DOI: 10.1021/acsami.8b09084
ACS Appl. Mater. Interfaces 2018, 10, 28672−28678

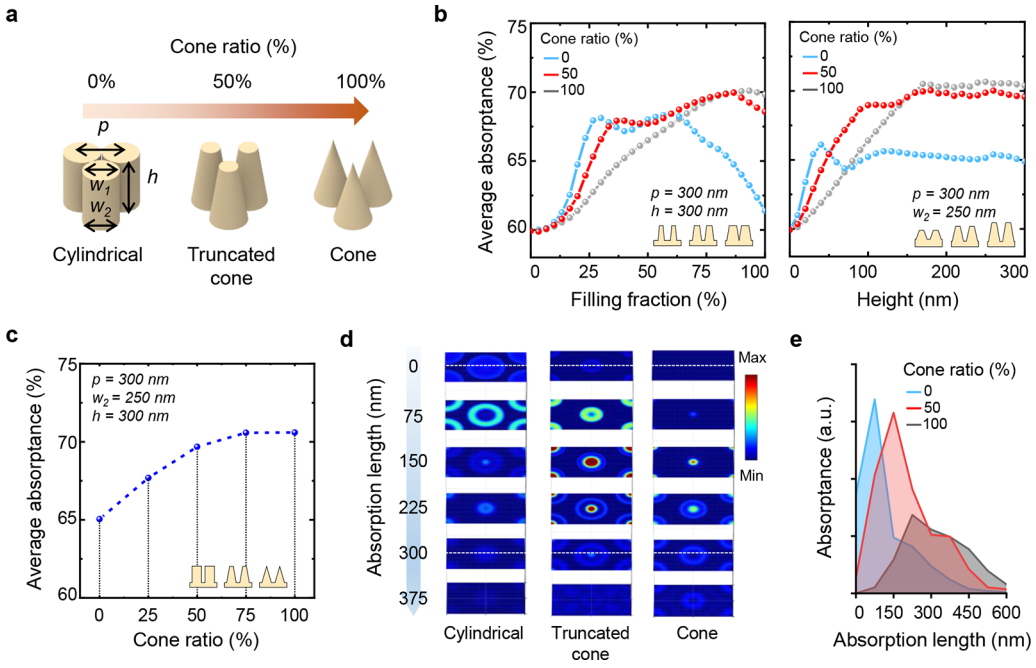

Figure 2. (a) Schematic view of GaN nanostructures and (b) Simulation results of average absorptance for GaN nanostructure as a function of filling fraction (FF), height in a wavelength range from 300 to 400 nm. (c) Simulation results of average absorptance for GaN nanostructure as a function of cone ratio in the wavelength range from 300 to 400 nm. (d) Absorption profiles in XY plane for cylindrical, truncated cone and cone structure at 350 nm wavelength and (e) light absorption length results from the absorption profiles.

conducted using a potentiostat (PARSTAT 4000A) at a scan rate of 10 mV/s. EIS was conducted at an applied potential of 1.23 V vs RHE. IPCE was measured using a potentiostat (nStat, Ivium Technologies).

RESULTS AND DISCUSSION

Figure 1a exhibits the configuration of the photoelectrochemical cell, which consists of quartz cell with a three electrode system with a working electrode (GaN photoanode), a counter electrode (Pt wire), and a reference electrode (Ag/AgCl electrode) in the electrolyte. To fabricate the truncated nanocones, the thermally dewetted metal was adopted for low cost and large area fabrication. A photograph and images of the GaN nanostructure fabricated by 15 min etched SiO_2 mask are presented in Figure 1b. The photograph after the etching process of GaN on a 2 in. substrate verifies that large-scale fabrication is possible. The GaN on a sapphire substrate shows the opaque properties due to strong light scattering from high refractive index and disordered structures.[25,26] The geometry information is shown in the SEM image (Figure 1b; inset); the height ~330 nm, the bottom width ~230 nm, and the top width ~100 nm with an angle of 82 degrees. The results of each GaN nanostructure according to the change of etching mask patterns are displayed in Supporting Information (SI) Figure S1.

We also simulated the electric field distribution by FDTD method at a wavelength of 350 nm in the case of planar and nanostructures on a sapphire substrate. The nanostructure geometries are cylindrical, truncated cone and cone shape with a top width of 250, 125, 0 nm respectively and a height of 300 nm, a period of 300 nm and a bottom width of 250 nm to demonstrate light propagation through the GaN nanostructures in the electrolyte condition (Figure 1c). The optical constant for the electrolyte was assumed to be the same as that of water. The electric field distributions for the GaN truncated nanocone show the concentration of light in the center of the nanostructure surrounded by the electrolyte compared to the other structures. Figure 1d exhibits simulated absorptance/reflectance spectra by RCWA calculation in the wavelength range from 300 to 400 nm for the GaN planar and truncated nanocone structures on sapphire substrate with a height and period of 300 nm, top width of 125 nm and a bottom width of 250 nm. In our computational study, all nanostructures were computed as hexagonal symmetry, according to previously reported disordered photonic structure calculations.[27−29] The schematics of simulation domain for GaN nanostructures are depicted in SI Figure S2. The truncated nanocone shows almost 100% absorptance and 0% reflectance. From the result of the optical simulations, the truncated nanocone absorbs light perfectly with respect to band gap energy ~3.4 eV and the photocatalytic performance for photocurrent density was enhanced by introducing the truncated nanocone, as shown in Figure 1e.

Figure 2a shows a schematic illustration of three representative GaN nanostructures, cylindrical, truncated cone, and cone arrays, for optical simulation. First, we defined the parameters such as period (p), height (h), top width (w_1), bottom width (w_2) and cone ratio (CR = $1 - w_2/w_1 \times 100\%$) to investigate the dependence of light absorption on the cone ratio, which was controlled by as follows: CR of 0, 50, and 100% correspond to the cylindrical, truncated cone, and cone structures, respectively. The absorption features of each structure are spectrally and spatially investigated (Figures 2b−d). Also, the geometrical parameters of all structures are identically configured for a thorough comparison: h is 300 nm, p is 300 nm, and w_2 is 250 nm (filling fraction = 83.3%). The bottom width, w_2, is set to 250 nm because it is identical with the minority diffusion length of the GaN to reduce the recombination rate.[18−20] We also simulated the nanostructure GaN in the electrolyte conditions. Figure 2b shows the average

DOI: 10.1021/acsami.8b09084
ACS Appl. Mater. Interfaces 2018, 10, 28672−28678

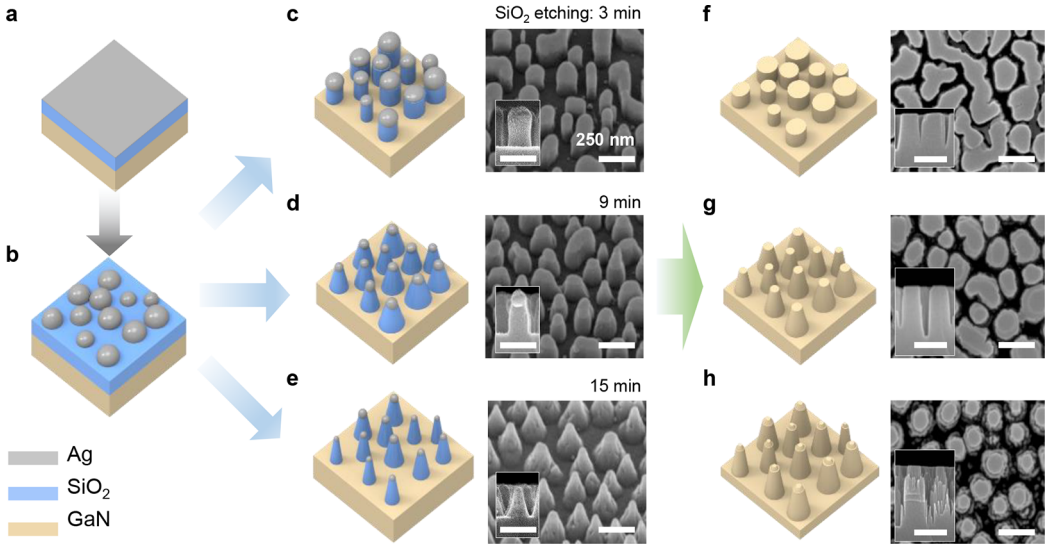

Figure 3. Schematic illustration of fabrication process steps for GaN truncated nanocones. (a) Deposition of SiO_2 (100 nm) and Ag (15 nm). (b) Formation of Ag nanoparticles with rapid thermal annealing process (c, d, e) 45-degree tilted view and cross-section (inset) SEM images of SiO_2 etching mask for 3, 9, 15 min with RIE and (f, g, h) Top-view and cross-section (inset) SEM images of GaN nanostructures under same etching conditions for 5 min with ICP-RIE. Scale bar is 250 nm.

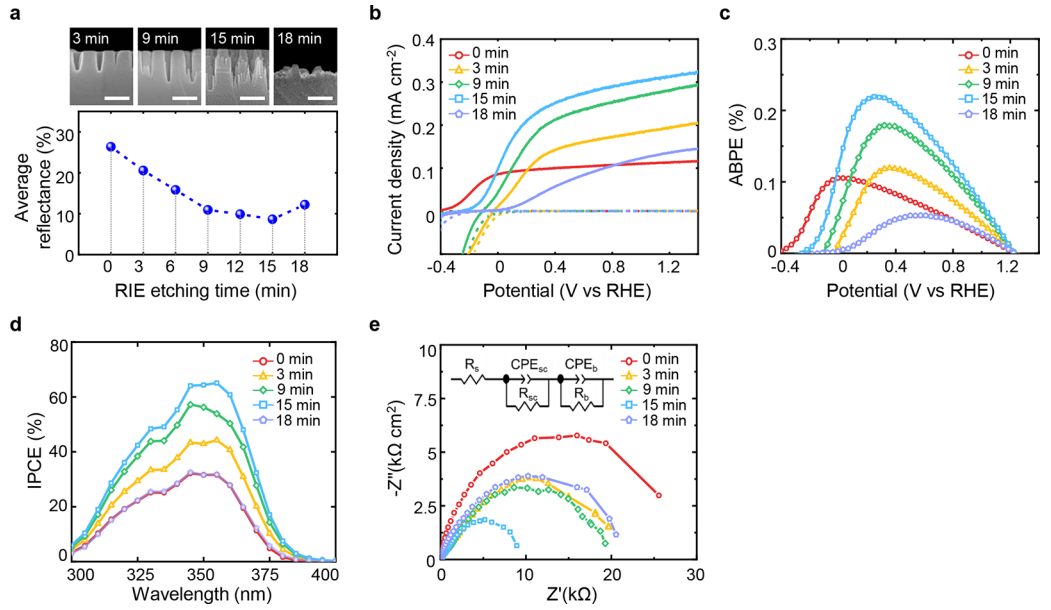

Figure 4. (a) SEM images of cross section views and average reflectance for planar GaN and truncated nanocones fabricated by 3, 9, 15, 18 min etched SiO_2 mask, respectively. Scale bar is 250 nm (b) Linear scan voltammetry for photocurrent density under dark (segment line) and illumination (straight line) conditions. (c) ABPE of the GaN photoanodes and (d) IPCE spectra under simulated light illumination at an applied potential of 1.23 V vs RHE. (e) EIS measurement and Nyquist plots of GaN photoanodes under illumination at an applied potential of 1.23 V vs RHE.

absorptance from RCWA results (SI Figure S3) as a function of the filling fraction and the height of the GaN structure with three CR values of 0, 50, and 100% (i.e., cylindrical, truncated cone, and cone), the cylindrical structure has a relatively poor absorption feature, below ~70%. In contrast, the truncated cone and cone prominently absorb the light >70%, when the height (h) is above 100 and 170 nm, respectively. and the filling fraction also has to be at least more than 60% as shown in Figure 2b. the absorptance saturates when the CR value has more than 50% in Figure 2c. However, most absorption in the cone structure occurs in the bulk rather than the nanostructure, and thereby many carriers generated by the photons are recombined. In this context, although the cone shows the best absorption characteristics, the truncated cone is an optimum structure for water-splitting because strong photon absorption is found at the center of GaN nanostructure (absorption depth = 150 nm) as shown in Figure 2d and e. The absorption profiles visualize this light trapping phenomenon of the truncated nanocone structure. Figure 2e exhibits the average absorptance of three representative morphologies as a function of absorption length. These spectral and spatial absorption analyses reveal that the truncated cone is the most appropriate geometry for water-splitting.

DOI: 10.1021/acsami.8b09084
ACS Appl. Mater. Interfaces 2018, 10, 28672−28678

Figure 3 shows the schematic process to fabricate the GaN truncated nanocones. First, Ag nanoparticles (NPs)/SiO_2 masks formed by rapid thermal annealing at 500 °C for 1 min with N_2 ambient of 200 mTorr. Then, as shown in Figures 3c–e, reactive ion etching (RIE, Oxford Plasmalab 80 Plus) was performed for 3, 9, and 15 min for various mask shapes (CF_4 flow/chamber pressure/temperature/RF power = 50 sccm/30 mTorr/23 °C/100 W).[30] As presented in Figure 3f–h, GaN was etched by inductively coupled plasma reactive ion etching (ICP-RIE, Oxford Plasmalab 100) using a Cl_2/Ar gas mixture. the ICP-RIE conditions are set identically for all GaN samples (Cl_2 flow/Ar flow/chamber pressure/temperature/RF power/ICP power/etching time = 20 sccm/10 sccm/10 mTorr/20 °C/100 W/600 W/5 min). After GaN etching, Ag NPs and SiO_2 residues were removed with nitric acid (HNO_3) and buffered oxide etcher (BOE) solution for 3 min, respectively. The GaN samples were cleaned using acetone, isopropyl alcohol (IPA) and deionized (DI) water and dried with N_2 blowing. As the geometry of SiO_2 goes from vertical rod to cone as shown in Figure 3c-e, GaN truncated nanocones with high aspect ratio are formed and nanopores are created on the surface of the nanostructure for the 15 min etched SiO_2 mask.

The average reflectance measured by a UV–visible spectrometer (SI Figure S4) for GaN samples with planar and truncated nanocone structures is plotted in Figure 4a. Comparing the results of previous simulations in Figure 1b, the absorptance was increased as the aspect ratio of the nanostructure increased in the cases of the truncated cone and cone structure, and the experimental data also shows similar results to those shown in SEM images. The flat surface of planar GaN shows reflectance value at ~26.3%. and the truncated nanocones with the high aspect ratio has the lowest average reflectance value at ~8.6% fabricated by the 15 min etched SiO_2 mask, in comparison with the other structures. the collapsed nanocone fabricated by the 18 min etched SiO_2 mask has also very low reflectance value at ~12% due to high degrees of surface roughness.[31,32]

For the photocatalytic performance, the photocurrent density of the truncated cone structure of GaN was measured as a function of the applied potential versus a reversible hydrogen electrode (V vs RHE) under dark and illumination conditions (Figure 4b). Dark currents were negligible for all GaN photoanodes. As a reference, the planar GaN photoanode was measured as 0.11 $mAcm^{-2}$ at 1.23 V vs RHE. The photocurrent densities for truncated nanocones fabricated by the 9 min, 15 min etched SiO_2 mask were 0.28 $mAcm^{-2}$ and 0.31 $mAcm^{-2}$ at 1.23 V vs RHE, respectively. The potential shifts toward higher for all GaN nanostructures with respect to planar GaN due to plasma etching damage.[18,34] Nevertheless, the enhancement of the photocurrent can be ascribed to the increase of the light absorption by truncated cone and a further increase of the surface area by the nanopores. In the case of the collapsed nanocone, even lower reflectance was obtained while the photocurrent density was lower below 0.8 V vs RHE compared to planar GaN. Consequently, the nanocone structure contributed to enhancement of the photocatalytic performance by charge carrier transport to the electrolyte. The applied bias photon to current efficiency (ABPE) was calculated (Figure 4c) for the GaN photoanode with planar and truncated nanocone structures according to eq 2. The maximum efficiency for the 15 min truncated nanocone photoanode is 0.22% at 0.24 V vs RHE, which is about 2.2 times higher than that of the planar GaN of 0.1% at −0.05 V vs RHE, and collapsed nanocone has the lowest value, ~0.5% at 0.6 V vs RHE

$$\mathrm{ABPE} = \frac{[J_{ph}(\mathrm{mAcm^{-2}}) \times (1.23 - V_{app}(\mathrm{V}))]}{P_{light}(\mathrm{mWcm^{-2}})} \times 100\% \quad (2)$$

The IPCE was measured using eq 3 to elucidate the improved efficiency of the incident photons conversion into charge carriers (Figure 4d). The IPCE spectra are given in Figure 4d, and the results show that the 15 min truncated nanocone exhibits the highest efficiency (~64.3%) compared to the planar GaN (~31.5%) at a wavelength of 350 nm and the efficiency decreased dramatically at wavelengths higher than 370 nm due to the bandgap energy (~3.4 eV).

$$\mathrm{IPCE} = \frac{J_{ph}(\mathrm{mAcm^{-2}}) \times 1240}{\lambda(\mathrm{nm}) \times P_{light}(\mathrm{mWcm^{-2}})} \times 100\% \quad (3)$$

Figure 4e shows the Nyquist plots from EIS measurement, which indicates the internal resistances corresponding to the overall charge transfer process with applied frequency from 10 000 to 0.1 Hz with static potential at 1.23 V vs RHE under light illumination. The semicircle at high frequency represents the charge transfer between the GaN nanostructure and electrolyte interfaces. The diameter of the semicircle is coincident with the charge transfer resistance.[35] In addition, the truncated nanocone with a high aspect ratio has the lowest diameter in the Nyquist plot. These results show that the charge recombination is reduced for the 15 min truncated nanocone. An equivalent circuit is presented in the inset of Figure 4e, and the values of constant phase elements and resistances are given in SI Table S1.

CONCLUSIONS

In summary, we have designed and fabricated GaN truncated nanocones for photocatalytic water splitting applications. The truncated nanocone was adopted to enhance the light trapping on the nanostructure with reduced light losses from the surface reflection. The absorptance for the truncated nanocone increased and saturated above a cone ratio of 50%, a height of 100 nm, and a filling fraction of 60%. Moreover, the incident light is concentrated inside the GaN nanostructure rather than inside the bulk, as simulated by a computational study. Consequently, it was experimentally found that the saturation of photocurrent increased around three times higher in the truncated nanocones compared to the planar GaN with a high incident photon to electron efficiency and charge transfer rate. In conclusion, the optimum truncated nanocone provides higher photocatalytic efficiency than the existing planar GaN-based water splitting by the only surface texturing without huge structural modification in the conventional system.[33] Furthermore, our proposed geometries with light trapping properties can also be applicable to GaN based photocatalytic materials. We believe our approach will pave a new way to improve the water splitting efficiency.

ASSOCIATED CONTENT

Supporting Information

The Supporting Information is available free of charge on the ACS Publications website at DOI: 10.1021/acsami.8b09084.

DOI: 10.1021/acsami.8b09084
ACS Appl. Mater. Interfaces 2018, 10, 28672–28678

SEM images of the samples; Simulation results of absorption spectra; Reflectance spectra of etched GaN samples; Fitting results of EIS analysis (PDF)

AUTHOR INFORMATION

Corresponding Author

*E-mail: ymsong@gist.ac.kr.

ORCID

Yeong Jae Kim: 0000-0002-0870-9044
Sanghan Lee: 0000-0002-5807-864X
Young Min Song: 0000-0002-4473-6883

Notes

The authors declare no competing financial interest.

ACKNOWLEDGMENTS

This work was supported by an Institute for Information & Communications Technology Promotion (IITP) grant funded by the Korea government (MSIP) (No.2017000709), The Creative Materials Discovery Program through the National Research Foundation of Korea (NRF) funded by the Korea government (MSIP) (NRF-2017M3D1A1039288) and Korea Basic Science Institute under the R&D program (Project No. D37615) supervised by the Ministry of Science.

REFERENCES

(1) Grätzel, M. Photoelectrochemical Cells. *Nature* **2001**, *414*, 338−344.

(2) Hisatomi, T.; Kubota, J.; Domen, K. Recent Advances in Semiconductors for Photocatalytic and Photoelectrochemical Water Splitting. *Chem. Soc. Rev.* **2014**, *43*, 7520−7535.

(3) Ebaid, M.; Kang, J. H.; Lim, S.-H.; Ha, J. S.; Lee, J. K.; Cho, Y. H.; Ryu, S. W. Enhanced Solar Hydrogen Generation of High Density, High Aspect Ratio, Coaxial InGaN/GaN Multi-Quantum Well Nanowires. *Nano Energy* **2015**, *12*, 215−223.

(4) Fujishima, A.; Honda, K. Electrochemical Photolysis of Water at a Semiconductor Electrode. *Nature* **1972**, *238*, 37−38.

(5) Schrauzer, G. N.; Guth, T. D. Photocatalytic Reactions. 1. Photolysis of Water and Photoreduction of Nitrogen on Titanium Dioxide. *J. Am. Chem. Soc.* **1977**, *99*, 7189−7193.

(6) Maeda, K.; Takata, T.; Hara, M.; Saito, N.; Inoue, Y.; Kobayashi, H.; Domen, K. GaN: ZnO Solid Solution as a Photocatalyst for Visible-Light-Driven Overall Water Splitting. *J. Am. Chem. Soc.* **2005**, *127*, 8286−8287.

(7) Yang, X.; Wolcott, A.; Wang, G.; Sobo, A.; Fitzmorris, R. C.; Qian, F.; Zhang, J. Z.; Li, Y. Nitrogen-Doped ZnO Nanowire Arrays for Photoelectrochemical Water Splitting. *Nano Lett.* **2009**, *9*, 2331−2336.

(8) Liu, R.; Lin, Y.; Chou, L. Y.; Sheehan, S. W.; He, W.; Zhang, F.; Hou, H. J. M.; Wang, D. Water Splitting by Tungsten Oxide Prepared by Atomic Layer Deposition and Decorated with an Oxygen-Evolving Catalyst. *Angew. Chem., Int. Ed.* **2011**, *50*, 499−502.

(9) Cole, B.; Marsen, B.; Miller, E.; Yan, Y.; To, B.; Jones, K.; Al-Jassim, M. Evaluation of Nitrogen Doping of Tungsten Oxide for Photoelectrochemical Water Splitting. *J. Phys. Chem. C* **2008**, *112*, 5213−5220.

(10) Tamirat, A. G.; Rick, J.; Dubale, A. A.; Su, W. N.; Hwang, B. J. Using Hematite for Photoelectrochemical Water Splitting: A Review of Current Progress and Challenges. *Nanoscale Horiz.* **2016**, *1*, 243−267.

(11) Kuykendall, T.; Ulrich, P.; Aloni, S.; Yang, P. Complete Composition Tunability of InGaN Nanowires Using a Combinatorial Approach. *Nat. Mater.* **2007**, *6*, 951.

(12) Benton, J.; Bai, J.; Wang, T. Enhancement in Solar Hydrogen Generation Efficiency Using a GaN-Based Nanorod Structure. *Appl. Phys. Lett.* **2013**, *102*, 173905−173904.

(13) Aryal, K.; Pantha, B. N.; Li, J.; Lin, J. Y.; Jiang, H. X. Hydrogen Generation by Solar Water Splitting Using p-InGaN Photoelectrochemical Cells. *Appl. Phys. Lett.* **2010**, *96*, 052110−052113.

(14) Maeda, K.; Teramura, K.; Saito, N.; Inoue, Y.; Domen, K. Photocatalytic Overall Water Splitting on Gallium Nitride Powder. *Bull. Chem. Soc. Jpn.* **2007**, *80*, 1004.

(15) Tao, T.; Zhi, T.; Liu, B.; Li, M.; Zhuang, Z.; Dai, J.; Li, Y.; Jiang, F.; Luo, W.; Xie, Z.; Chen, D.; Chen, P.; Li, Z.; Zou, Z. G.; Zhang, R.; Zheng, Y. Significant Improvements in InGaN/GaN Nanophotoelectrodes for Hydrogen Generation by Structure and Polarization Optimization. *Sci. Rep.* **2016**, *6*, 20218.

(16) Yang, C.; Xi, X.; Yu, Z.; Cao, H.; Li, J.; Lin, S.; Ma, Z.; Zhao, L. Light Modulation and Water Splitting Enhancement Using a Composite Porous GaN Structure. *ACS Appl. Mater. Interfaces* **2018**, *10*, 5492−5497.

(17) Ebaid, M.; Min, J. W.; Zhao, C.; Ng, T. K.; Idriss, H.; Ooi, B. S. Water Splitting to Hydrogen over Epitaxially Grown InGaN Nanowires on a Metallic Titanium/Silicon Template: Reduced Interfacial Transfer Resistance and Improved Stability to Hydrogen. *J. Mater. Chem. A* **2018**, *6*, 6922−6930.

(18) Narangari, P. R.; Karuturi, S. K.; Lysevych, M.; Tan, H. H.; Jagadish, C. Improved Photoelectrochemical Performance of GaN Nanopillar Photoanodes. *Nanotechnology* **2017**, *28*, 154001.

(19) Li, J.; Cushing, S. K.; Zheng, P.; Meng, F.; Chu, D.; Wu, N. Plasmon-Induced Photonic and Energy-Transfer Enhancement of Solar Water Splitting by a Hematite Nanorod Array. *Nat. Commun.* **2013**, *4*, 2651.

(20) Wang, K. X.; Yu, Z.; Liu, V.; Brongersma, M. L.; Jaramillo, T. F.; Fan, S. (2014). Nearly Total Solar Absorption in Ultrathin Nanostructured Iron Oxide for Efficient Photoelectrochemical Water Splitting. *ACS Photonics* **2014**, *1*, 235−240.

(21) Qiu, Y.; Liu, W.; Chen, W.; Chen, W.; Zhou, G.; Hsu, P.-C.; Zhang, R.; Liang, Z.; Fan, S.; Zhang, Y. Efficient Solar-Driven Water Splitting by Nanocone $BiVO_4$-Perovskite Tandem Cells. *Sci. Adv.* **2016**, *2*, e1501764.

(22) Jeong, S. Y.; Shin, H. M.; Jo, Y. R.; Kim, Y. J.; Kim, S. K.; Lee, W. J.; Lee, G. J.; Song, J. S.; Moon, B. J.; Seo, S. H.; An, H. J.; Lee, S. H.; Song, Y. M.; Kim, B. J.; Yoon, M. H.; Lee, S. H. Plasmonic Silver Nanoparticle-Impregnated Nanocomposite $BiVO_4$ Photoanode for Plasmon-Enhanced Photocatalytic Water Splitting. *J. Phys. Chem. C* **2018**, *122*, 7088−7093.

(23) Yang, C.; Liu, L.; Zhu, S. C.; Yu, Z. G.; Xi, X.; Wu, S. T.; Cao, H. C.; Li, J. M.; Zhao, L. X. GaN with Laterally Aligned Nanopores to Enhance the Water Splitting. *J. Phys. Chem. C* **2017**, *121*, 7331−7336.

(24) Song, Y. M.; Choi, E. S.; Park, G. C.; Park, C. Y.; Jang, S. J.; Lee, Y. T. Disordered Antireflective Nanostructures on GaN-Based Light-Emitting Diodes Using Ag Nanoparticles for Improved Light Extraction Efficiency. *Appl. Phys. Lett.* **2010**, *97*, 093110.

(25) Song, Y. M.; Jang, J. H.; Lee, J. C.; Kang, E. K.; Lee, Y. T. Disordered Submicron Structures Integrated on Glass Substrate for Broadband Absorption Enhancement of Thin-Film Solar Cells. *Sol. Energy Mater. Sol. Cells* **2012**, *101*, 73−78.

(26) Haghanifar, S.; Gao, T.; De Vecchis, R. T. R.; Pafchek, B.; Jacobs, T. D.; Leu, P. W. Ultrahigh-Transparency, Ultrahigh-Haze Nanograss Glass with Fluid-Induced Switchable Haze. *Optica* **2017**, *4*, 1522−1525.

(27) Choi, K.; Park, S. H.; Song, Y. M.; Lee, Y. T.; Hwangbo, C. K.; Yang, H.; Lee, H. S. Nano-Tailoring the Surface Structure for the Monolithic High-Performance Antireflection Polymer Film. *Adv. Mater.* **2010**, *22*, 3713−3718.

(28) Song, Y. M.; Choi, H. J.; Yu, J. S.; Lee, Y. T. Design of Highly Transparent Glasses with Broadband Antireflective Subwavelength Structures. *Opt. Express* **2010**, *18*, 13063−13071.

(29) Pratesi, F.; Burresi, M.; Riboli, F.; Vynck, K.; Wiersma, D. S. Disordered Photonic Structures for Light Harvesting in Solar Cells. *Opt. Express* **2013**, *21*, A460−A468.

(30) Dewan, R.; Shrestha, S.; Jovanov, V.; Hüpkes, J.; Bittkau, K.; Knipp, D. Random Versus Periodic: Determining Light Trapping of Randomly Textured Thin Film Solar Cells by the Superposition of

DOI: 10.1021/acsami.8b09084
ACS Appl. Mater. Interfaces 2018, 10, 28672−28678

Periodic Surface Textures. *Sol. Energy Mater. Sol. Cells* **2015**, *143*, 183−189.
(31) Ji, S.; Park, J.; Lim, H. Improved Antireflection Properties of Moth Eye Mimicking Nanopillars on Transparent Glass: Flat Antireflection and Color Tuning. *Nanoscale* **2012**, *4*, 4603−4610.
(32) Bennett, H. E.; Porteus, J. O. Relation Between Surface Roughness and Specular Reflectance at Normal Incidence. *J. Opt. Soc. Am.* **1961**, *51*, 123−129.
(33) Benzarti, Z.; Khelifi, M.; Halidou, I.; El Jani, B. Study of Surface and Interface Roughness of GaN-Based Films Using Spectral Reflectance Measurements. *J. Electron. Mater.* **2015**, *44*, 3243−3252.
(34) Tseng, W. J.; van Dorp, D. H.; Lieten, R. R.; Vereecken, P. M.; Langer, R.; Borghs, G. Impact of Plasma-Induced Surface Damage on the Photoelectrochemical Properties of GaN Pillars Fabricated by Dry Etching. *J. Phys. Chem. C* **2014**, *118*, 11261−11266.
(35) Lopes, T.; Andrade, L.; Ribeiro, H. A.; Mendes, A. Characterization of Photoelectrochemical Cells for Water Splitting by Electrochemical Impedance Spectroscopy. *Int. J. Hydrogen Energy* **2010**, *35*, 11601−11608.

DOI: 10.1021/acsami.8b09084
ACS Appl. Mater. Interfaces 2018, 10, 28672−28678